


RESEARCH

Open Access



Doxorubicin synergizes bortezomib-induced multiple myeloma cell death by inhibiting aggresome formation and augmenting endoplasmic reticulum/Golgi stress and apoptosis

Chang-Tze Ricky Yu¹, Yu-Ting Amber Liao¹, Chi-Yin Nina Chiang¹, Jo-Mei Maureen Chen¹, Hsin-Yu Bella Pan¹, Chia-Yun Pan¹, Wei-Jun Jiang¹, Jia-Rung Tsai², Tsung-Ying Yang^{3,4} and Chieh-Lin Jerry Teng^{2,5,6,7,8,9*} 

Abstract

Background Bortezomib is a standard treatment for multiple myeloma (MM), working by the accumulation of toxic misfolded proteins in cancer cells. However, a significant clinical challenge arises from the development of resistance to bortezomib in MM treatment. Aggresome, a subcellular structure enclosed within Vimentin, forms in response to proteasome inhibitors and sequesters misfolded proteins that are transported by histone deacetylase 6 (HDAC6) and Dynein for degradation via autophagy, thereby reducing bortezomib's cytotoxic effects. Therefore, in this study, we screened several anticancer agents to identify those that could synergize with bortezomib to enhance cell death and block aggresome formation in the MM cell line U266B1.

Methods To enhance bortezomib's efficacy, we screened a range of anticancer compounds for their potential to promote cell death and inhibit aggresome formation in U266B1 MM cells. We utilized the trypan blue exclusion assay and immunofluorescence for evaluation, and explored the underlying mechanisms through Western blot analysis.

Results Doxorubicin enhanced bortezomib-induced cytotoxicity while inhibiting aggresome formation. Mechanistic studies revealed that doxorubicin downregulated key aggresome components, including Vimentin, HDAC6, and Dynein, leading to accumulation of misfolded proteins and augmentation of proapoptotic and necroptotic pathways by intensifying endoplasmic reticulum (ER) and Golgi stress responses. Notably, doxorubicin did not enhance cell death triggered by proteasome inhibitors that do not induce aggresome formation. Furthermore, the combination of bortezomib and doxorubicin failed to produce synergy in the killing of MM cell lines that lacked aggresome-forming ability.

Conclusions Doxorubicin enhances bortezomib-induced cell death in MM by inhibiting aggresome formation and amplifying ER/Golgi stress and apoptosis. This study highlights the potential therapeutic benefits of combining bortezomib with doxorubicin for MM treatment.

Keywords Bortezomib, Doxorubicin, Multiple myeloma, Aggresome, Golgi stress

*Correspondence:

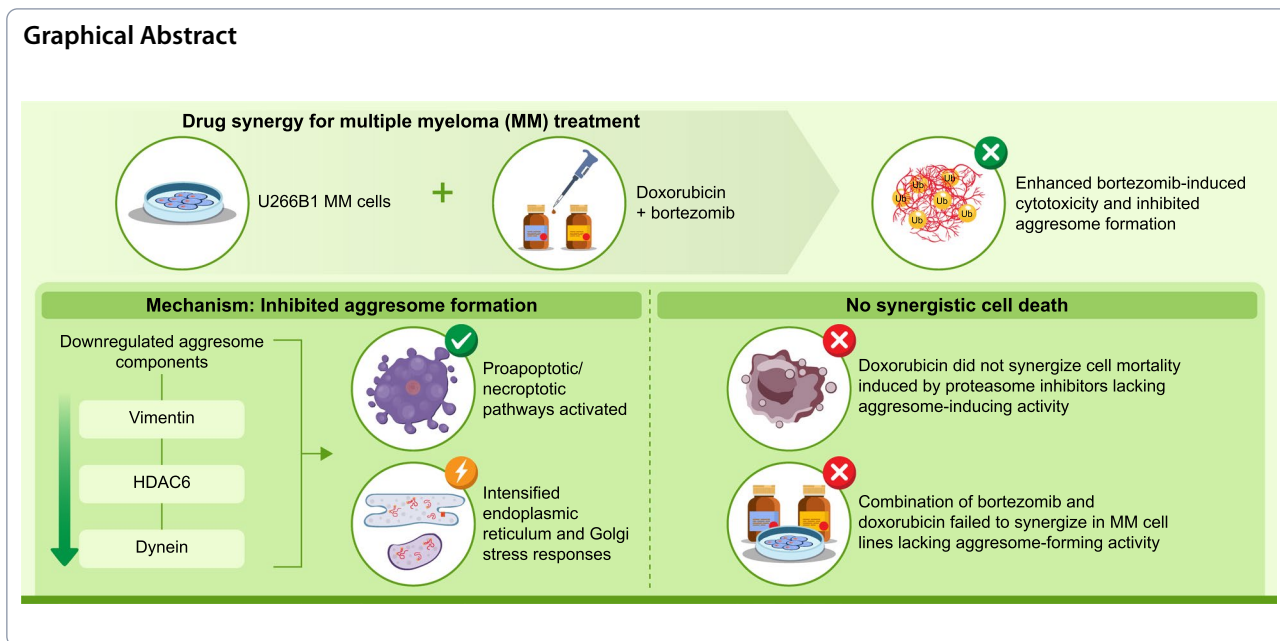
Chieh-Lin Jerry Teng
drteng@vghtc.gov.tw

Full list of author information is available at the end of the article



© The Author(s) 2024. **Open Access** This article is licensed under a Creative Commons Attribution-NonCommercial-NoDerivatives 4.0 International License, which permits any non-commercial use, sharing, distribution and reproduction in any medium or format, as long as you give appropriate credit to the original author(s) and the source, provide a link to the Creative Commons licence, and indicate if you modified the licensed material. You do not have permission under this licence to share adapted material derived from this article or parts of it. The images or other third party material in this article are included in the article's Creative Commons licence, unless indicated otherwise in a credit line to the material. If material is not included in the article's Creative Commons licence and your intended use is not permitted by statutory regulation or exceeds the permitted use, you will need to obtain permission directly from the copyright holder. To view a copy of this licence, visit <http://creativecommons.org/licenses/by-nc-nd/4.0/>.

Graphical Abstract



Introduction

Cancer cells tend to produce large quantities of misfolded proteins owing to gene mutations, aneuploidy, or stressful conditions within the tumor microenvironment [1]. These misfolded proteins can exert toxicity on cells by causing loss of function of the abnormally folded proteins [2], disrupting cellular processes by creating spatial obstacles [3], binding to and permeabilizing biomembranes [4], inducing oxidative stress, and activating apoptosis via the unfolded protein response [5]. Consequently, chemical inhibition of the proteasome—the primary subcellular structure responsible for degrading misfolded proteins, has emerged as a therapeutic strategy in cancer treatment [6].

However, chemically inactivating the proteasome causes the rapid buildup of misfolded proteins, which are often polyubiquitylated and recognized by several factors, including Histone Deacetylase 6 (HDAC6) [7], the Heat Shock Protein 70 (HSP70)/Bcl-2-associated athanogene 3 (BAG3)/14-3-3 protein complex [8], eukaryotic Elongation Factor 1 Alpha 1 (eEF1A1), and Dynactin Subunit 1 (DCTN1) [9]. These factors bind to the misfolded proteins and transport them via dynein to the cell center, where the vimentin network reorganizes into a cage-like structure that sequesters the toxic ubiquitylated misfolded proteins. These sequestered proteins are then degraded through autophagy [10]. Hence, the formation of aggresomes may attenuate the cytotoxicity induced by proteasome inhibitors.

Inhibiting the proteasome and the aggresome results in a synergistic effect, significantly enhancing the

destruction of cancer cells, particularly in multiple myeloma (MM) [11]. Therefore, disrupting aggresome is considered a promising strategy to boost the cytotoxicity induced by proteasome inhibitors. However, few compounds have been reported to possess aggresome-inhibitory activity [12]. Multiple myeloma is a blood malignancy arising from monoclonal plasma cells. It typically presents with symptoms such as anemia, bone pain, hypercalcemia, and renal dysfunction and accounts for approximately 19% of all hematological cancers [13]. Combinations of proteasome inhibitors, immunomodulatory drugs, and dexamethasone are the current standard treatment for newly diagnosed MM [14]. Among the available proteasome inhibitors, bortezomib has been widely utilized in diverse MM treatment regimens. Bortezomib is a dipeptide boronic acid inhibitor that effectively inhibits proteasome activity by specifically targeting the beta-1 and beta-5 subunits, with minimal effects on other proteases [15]. This inhibition causes the accumulation of misfolded proteins, making bortezomib particularly effective in MM treatment owing to the high level of protein production in MM cells [16]. However, the efficacy of bortezomib has been undermined by the development of drug resistance in MM, with aggresome formation playing a pivotal role [17].

In this study, we screened several anticancer agents to identify those that could synergize with bortezomib to enhance cell death in the MM cell line U266B1. Doxorubicin, a widely used anticancer drug with diverse pharmacological effects, including in the treatment of MM, was found to enhance bortezomib-induced cell death

and inhibit bortezomib-induced aggresome formation synergistically. Mechanistic analyses revealed that doxorubicin downregulated key aggresome-promoting factors, such as Vimentin, HDAC6, eEF1A1, and dynein, whereas simultaneously activating pathways related to endoplasmic reticulum (ER) or Golgi stress responses and apoptosis. Notably, doxorubicin did not potentiate cell death triggered by proteasome inhibitors that lacked aggresome-stimulating activity. Furthermore, the combination of bortezomib and doxorubicin failed to induce synergistic cell death in the MM cell lines without aggresome-forming potential. These findings suggest that doxorubicin enhances bortezomib-induced cell death by inhibiting aggresome formation, thereby augmenting ER and Golgi stress responses and further enhancing apoptosis.

Materials and methods

Chemicals, reagents and antibodies

Roswell Park Memorial Institute (RPMI) 1640 medium, penicillin, streptomycin, and trypan blue were purchased from GIBCO (Bethesda, MD, USA), whereas fetal bovine serum was sourced from Cytiva (Marlborough, MA, USA). Bortezomib, doxorubicin, lenalidomide, pomalidomide, dexamethasone, alisertib, regorafenib, gemcitabine, clioquinol, capzimin, 3-methyladenine (3-MA), vacuolar protein sorting 34-phosphatidylinositol 3-kinase III (Vps34-PIK III), chloroquine, and MHY1485 were obtained from MedChemExpress (Monmouth Junction, NJ, USA), and EPZ015666 was sourced from Sigma (St. Louis, MO, USA). All cell lines, including U266B1, RPMI-8226, and NCI-H929, were purchased from the American Type Culture Collection. Antibodies against cellular myelocytomatosis (c-Myc) (A19032), sequestosome-1 (p62) (A19700), nuclear factor erythroid 2-related factor 2 (NRF2) (A3577), HSP70 (A12948), BAG3 (A14826), 14-3-3 γ (A9162), 14-3-3 ϵ (A4933), 14-3-3 ζ (A7639), eEF1A1 (A11545), hook microtubule-tethering protein 2 (HOOK2) (A9337), DCTN1 (A1783), dynein light chain LC8-type 1 (DYNLL1) (A14496), dynein axonemal heavy chain 5 (DNAH5) (A17472), autophagy-related 4C cysteine peptidase (ATG4C) (A7396), microtubule-associated proteins 1A/1B light chain 3B (A19665), HSP90 β (A21799), inositol-requiring enzyme 1 (IRE1) (A21021), phosphorylated IRE1 serine 724 (pIRE S724) (AP1442), glucose-regulated protein 78 (GRP78) (A11366), C/EBP homologous protein (CHOP) (A0221), activating transcription factor 3 (ATF3) (A13469), ATF4 (A18687), ADP-ribosylation factor 4 (ARF4) (A7644), cyclic AMP-responsive element-binding protein 3 (CREB3) (A6567), E26 transformation-specific sequence 1 (ETS1) (A15666), ETS2 (A7329), and HSP47 (A13474) were purchased from Abclonal (Woburn, MA, USA). Antibodies against

p-38 (#8690P), phosphorylated-p38 (#4511P), Bcl-2-associated death promoter (Bad) (#9239), phosphorylated Bad serine 112 (#5284), Bcl-2-associated X protein (Bax) (#5023), Bcl-2-interacting killer (Bik) (#4592), Bcl-2-interacting mediator of cell death (Bim) (#2933), BH3-interacting domain death agonist (BID) (#2002), Bcl-2 homologous antagonist/killer (Bak) (#12105), p53 upregulated modulator of apoptosis (Puma) (#12450), Caspase 3 (#14220), cleaved Caspase 3 (#9664), Caspase 7 (#12827), cleaved Caspase 7 (#8438), Caspase 9 (#9508), cleaved Caspase 9 (#52873), poly(ADP-ribose) polymerase (PARP) (#9542), cleaved PARP (#5625), receptor-interacting serine/threonine-protein kinase 1 (RIPK1) (#3493), mixed lineage kinase domain-like protein (#14993), and RIPK3 (#13526) were obtained from Cell Signaling Technology (Danvers, MA, USA). The antibody against 14-3-3 η (sc-17287) was purchased from Santa Cruz Biotechnology (Dallas, TX, USA), whereas the dynein antibody (MA1-070) was sourced from Invitrogen (Carlsbad, CA, USA). Various horseradish peroxidase (HRP)-conjugated secondary antibodies were purchased from Cell Signaling Technology (Danvers, MA, USA), and HRP substrates were obtained from Advanta (San Jose, CA, USA)."

Cell culture

The U266B1, RPMI-8226, and NCI-H929 MM cell lines were cultured at 37 °C in 5% CO₂ using RPMI 1640 medium with 2 mM L-glutamine, 100 U/mL penicillin, and 100 μ g/mL streptomycin. Specific conditions were as follows: (i) U266B1 cells were grown in medium containing 15% fetal bovine serum and 1.5 g/L sodium bicarbonate; (ii) RPMI-8226 cells were maintained in medium supplemented with 20% fetal bovine serum, 1.5 g/L sodium bicarbonate, 4.5 g/L glucose, 10 mM HEPES, and 1 mM sodium pyruvate; (iii) NCI-H929 cells were cultured in medium with 10% fetal bovine serum, 2 g/L sodium bicarbonate, and 1 mM sodium pyruvate.

Preparation of cell extracts and Western blot

To prepare cell-free extracts, cells were lysed using a buffer made of 50% lysate buffer and 50% IP washing buffer. The lysate buffer contained 20 mM PIPES (pH 7.2), 100 mM NaCl, 1 mM EDTA, 0.1% CHAPS, 10% sucrose, 1 mM PMSF, 1 mM DTT, 1 mM sodium orthovanadate, and 10 μ g/mL of protease inhibitors (leupeptin, aprotinin, chymostatin, pepstatin). The IP washing buffer consisted of 10 mM HEPES (pH 7.6), 2 mM magnesium chloride, 50 mM NaCl, 5 mM EGTA, 0.1% Triton X-100, and 40 mM β -glycerophosphate. Lysates were incubated at 4 °C for 30 min. Cellular debris was removed by centrifuging at 13,000 rpm for 90 min in an Eppendorf centrifuge. Protein concentration in the

supernatants was determined with the Bradford assay (BIO-RAD, Richmond, CA, USA). For analysis, 50–100 µg of protein was heated to 95 °C for 10 min. Samples were loaded onto a 10% SDS-PAGE gel and transferred to a PVDF membrane (Millipore, Bedford, MA). The PVDF membrane was blocked with 5% BSA in PBST (0.1% Tween 20 in PBS). Primary antibodies were incubated with the membrane overnight at 4 °C. Membranes were washed three times with PBST for 30 min each at room temperature. Secondary antibodies conjugated to HRP were added for 1 h at room temperature. The membrane was washed again with PBST three times for 30 min each. Finally, HRP substrates were applied to develop the membrane.

Immunofluorescence

Cells grown on polylysine-coated coverslips or mounted on slides via cytospin were washed with PBS and fixed in cold methanol at –20 °C for 20 min. Fixed cells were incubated with primary antibodies for 1 h at room temperature. Afterward, they were washed three times with TBST (tris-buffered saline with 0.1% Tween 20).

Secondary antibodies conjugated with TRITC or FITC, together with DAPI, were added for 1 h. The samples were washed again with TBST. Finally, they were mounted in 90% glycerol containing *p*-phenylenediamine as an anti-fading reagent. Fluorescence images were captured using a fluorescence microscope from Olympus Optical Co., Ltd (Tokyo, Japan).

Cell mortality assay

Cell viability was assessed using a trypan blue exclusion assay. In this procedure, cells were incubated with a 0.2% solution of trypan blue, loaded onto a hemocytometer, and examined under a microscope. Cells that stained blue were classified as non-viable.

Statistical analysis

Regarding drug synergy, synergism occurs when the combination of two or more agents produces effects more than the sum of the individual effects [18]. We defined synergistic cell death as a significantly greater level of cell mortality induced by the combination of bortezomib and doxorubicin compared to the sum of cell death caused by bortezomib alone and doxorubicin alone. For other statistical analyses, we used SPSS software (version 22.0; SPSS Inc., Chicago, IL, USA). Depending on the context, either one-way ANOVA followed by Tukey's post hoc test for multiple comparisons or t-tests or were performed. Statistical significance was defined as a P-value < 0.05.

Results

Doxorubicin synergized bortezomib-induced cell death in U266B1 cells

We initially screened a range of anticancer agents for their potential to enhance bortezomib-induced cell death in the MM cell line U266B1. This screening included two anticancer drugs, gemcitabine and regorafenib; four drugs commonly used in the treatment of MM, including lenalidomide, pomalidomide, dexamethasone, and doxorubicin; furthermore, two experimental anti-MM compounds, EPZ01566 and alisertib. Bortezomib was administered at a concentration of 6.25 nM, which led to approximately 30–40% cell death. The test compounds, each used at concentrations inducing 10–20% cell death, were added individually or in combination with bortezomib. Cell viability was assessed 24 h later using the trypan blue exclusion assay. The results indicated that only doxorubicin produced synergistic cell death when combined with bortezomib. This is evidenced by a significantly higher observed cell death rate with the combination treatment (experimental death value, E) compared to the sum of the cell death rates from bortezomib and doxorubicin (theoretical additive value, T) (Fig. 1). In contrast, the other compounds either produced an additive effect with bortezomib (E approximately equal to T) or failed to achieve an additive effect ($E < T$).

Doxorubicin inhibits bortezomib-induced aggresome formation in U266B1 cells

We then investigated whether doxorubicin could inhibit aggresome formation. Given the limited scientific evidence on aggresome formation in cancerous B cells, we aimed to characterize this process in the MM cell line U266B1. U266B1 cells were treated with bortezomib for various durations, and immunofluorescence analysis using antibodies against Vimentin and Ubiquitin, two key aggresome markers, was performed. As shown in Fig. 2A, Vimentin in the U266B1 cells before drug treatment exhibited either a larger circular cage, a blurred cage, or a dispersed pattern. Upon increasing the bortezomib incubation period, the percentage of cells exhibiting larger cages or dispersed Vimentin decreased, whereas the percentage of cells with blurred or small, dense cages gradually increased (Fig. 2B). Conversely, ubiquitin was undetectable in U266B1 cells prior to treatment; however, small ubiquitin aggregates began to form at 6 h, followed by a major aggregate at 12 h of bortezomib treatment (Figs. 2A, C). Since aggresomes are clusters of ubiquitinated misfolded proteins enclosed by a Vimentin cage [10], we monitored the progression of ubiquitin signals within blurred (Fig. 2D) or small Vimentin cages (Fig. 2E). Initially, ubiquitin signals were either dispersed

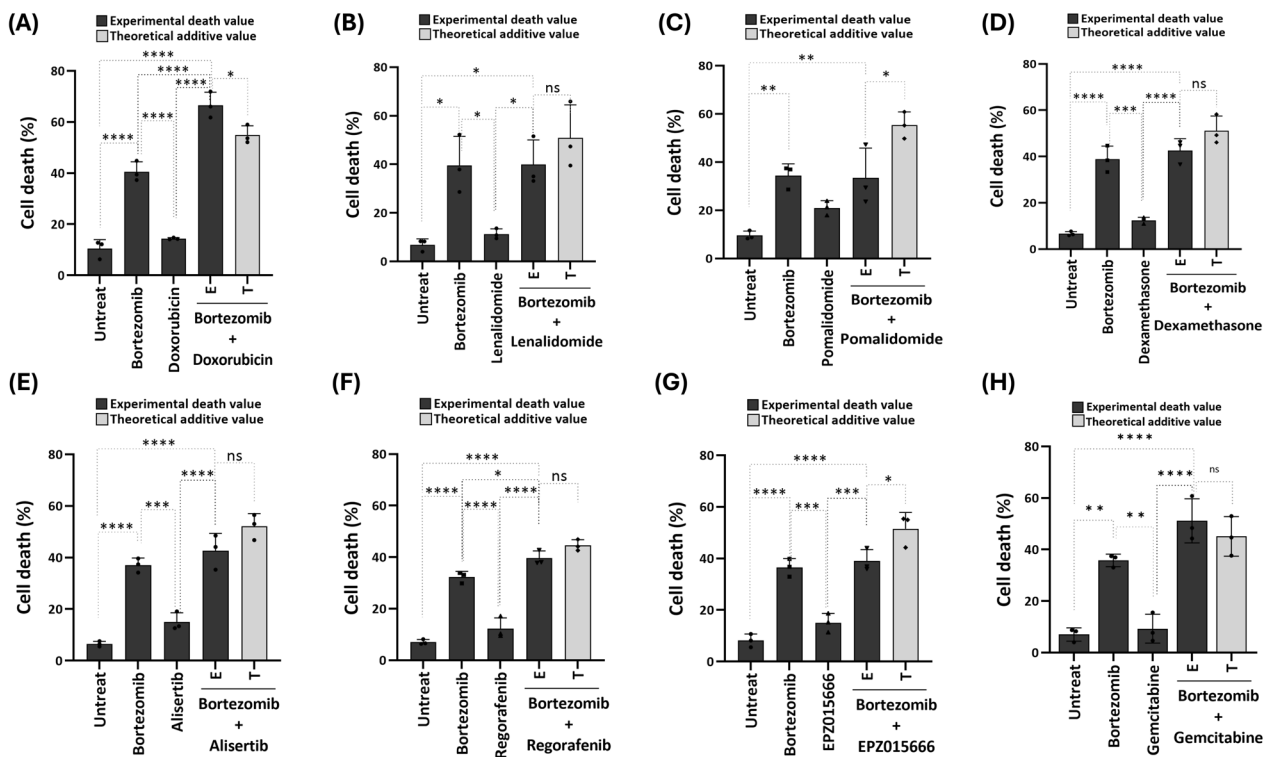


Fig. 1 Doxorubicin synergized with bortezomib to induce cell death in U266B1 cells. U266B1 cells were treated with either no compound, 6.25 nM Bortezomib, or one of the following compounds: 12.5 μg/ml Gemcitabine (A), 10 μM Alisertib (B), 10 μM Regorafenib (C), 20 μM EPZ015666 (D), 10 μM Lenalidomide (E), 10 μM Pomalidomide (F), 10 μM Dexamethasone (G), 1 μM Doxorubicin (H), or a combination of bortezomib with one of the listed compounds. After 24 h, trypan blue exclusion assays were conducted to assess cell death. At these concentrations, bortezomib induced 30–40% cell death, whereas each tested compound resulted in 10–20% cell death. The experimental death value (E) represents the observed cell death resulting from the combination treatment, whereas the theoretical additive value (T) represents the sum of cell death induced by each drug individually. Statistical significance was determined using one-way ANOVA followed by Tukey’s multiple comparison test, with p-values of <0.05 (*), <0.01 (**), <0.001 (***), and <0.0001 (****); ns indicates no significance. All experiments were performed independently three times

or undetectable in cells before treatment (Type A); however, as bortezomib treatment progressed, an increasing number of cells displayed multiple separated ubiquitin particles within the Vimentin cage by 6 h (Type B). By 12 h, these aggregates began to merge (Type C) and soon after fused into a single, compact cluster within the

Vimentin cage (Type D). Thus, during the early hours of bortezomib treatment, ubiquitinated misfolded proteins exhibit a Type B distribution within the Vimentin cage, transitioning almost simultaneously to Types C and D. Ultimately, we defined aggresome in U266B1 cells as either multiple closely clustered ubiquitin aggregates

(See figure on next page.)

Fig. 2 Doxorubicin blocks bortezomib-induced aggresome formation in U266B1 cells. **A–C** Characterization of the formation of Vimentin cages and the aggregation of ubiquitinated misfolded proteins during aggresome formation. U266B1 cells were treated with 6.25 nM bortezomib for 0–24 h and analyzed by immunofluorescence to observe Vimentin and Ubiquitin (A). The percentage of cells with different forms of Vimentin (B) or Ubiquitin (C) was quantified and plotted. **D, E** Kinetics of Ubiquitin changes in cells with blurred or small Vimentin cages. U266B1 cells treated with 6.25 nM Bortezomib for 0–24 h were analyzed by immunofluorescence to observe Vimentin and Ubiquitin. The distribution of Ubiquitin in cells with blurred Vimentin cages (D) or small Vimentin cages (E) was quantified and plotted. Ubiquitin distribution was classified as: A, dispersed Ubiquitin; B, separated Ubiquitin particles; C, closely packed Ubiquitin particles; D, compact, clustered Ubiquitin. **F** Bortezomib stimulates aggresome formation in U266B1 cells. Cells were treated with 6.25 nM Bortezomib for 0–24 h, and immunofluorescence was used to observe Vimentin and Ubiquitin. Aggresomes were defined as Ubiquitin in type C or D, enclosed by blurred or small Vimentin cages. **G** Doxorubicin inhibits Bortezomib-induced aggresome formation. U266B1 cells were treated with no compound, 6.25 nM Bortezomib, 1 μM Doxorubicin, or the combination for 18 h, followed by immunofluorescence analysis for Vimentin and Ubiquitin. The percentage of cells with aggresomes, as defined in (F), was quantified and plotted. Statistical significance was determined by one-way ANOVA with Tukey’s multiple comparison test: *p < 0.05, ***p < 0.001. All experiments were performed independently three times. Scale bar: 10 μm

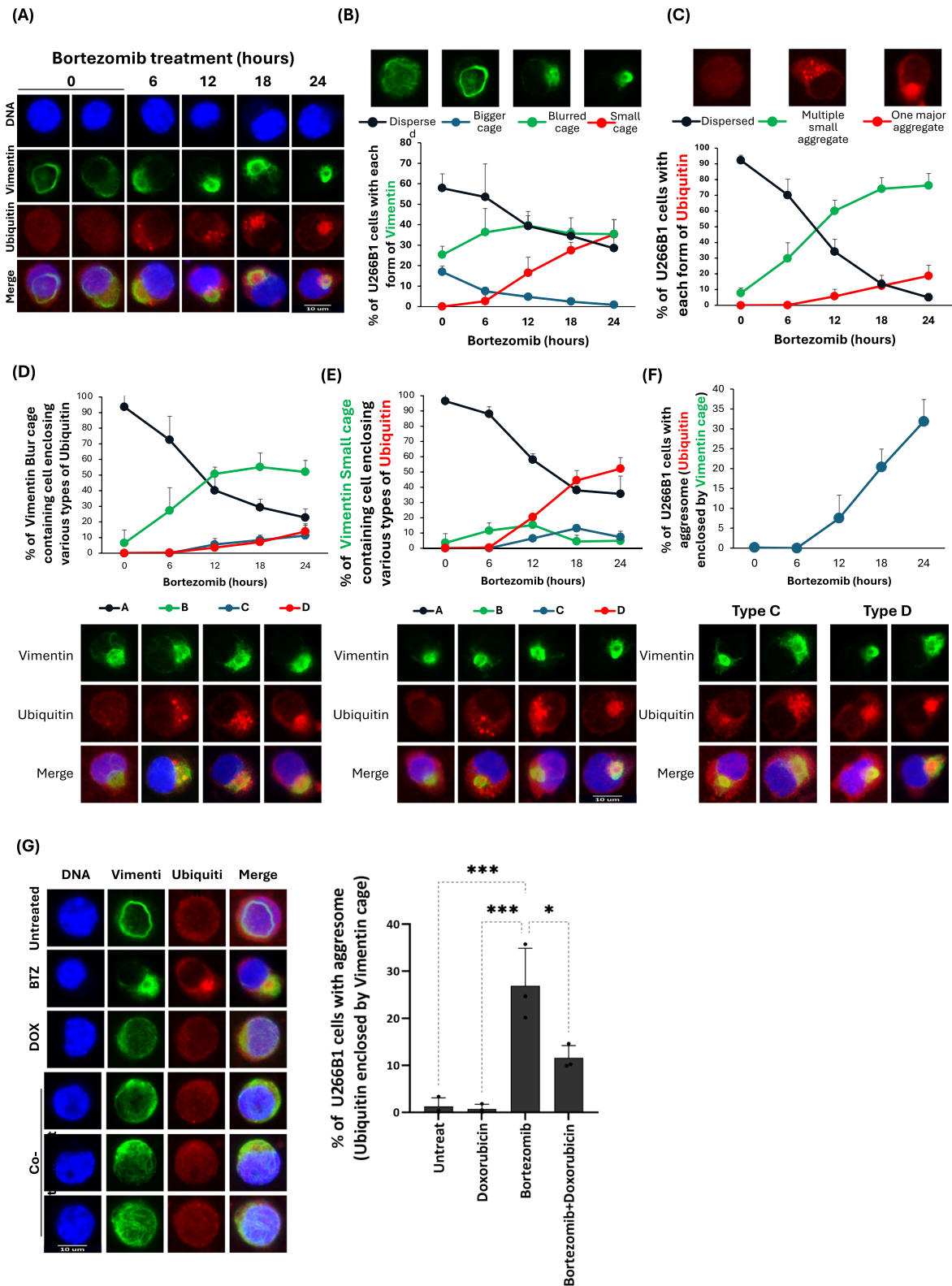


Fig. 2 (See legend on previous page.)

(Type C) or a single major ubiquitin cluster (Type D) enclosed by a blurred or small Vimentin cage. Notably, U266B1 cells rapidly and steadily formed aggresomes upon continuous bortezomib exposure, with more than 30% of cells exhibiting aggresomes in their cytoplasm after 24 h (Fig. 2F).

Next, we assessed whether doxorubicin could block bortezomib-induced aggresome formation. U266B1 cells were treated with bortezomib and doxorubicin either individually or combined for 18 h—a shorter duration compared with 24 h to retain more viable cells on the coverslips. We found that co-treatment with doxorubicin significantly reduced aggresome formation in bortezomib-treated cells (Fig. 2G).

Doxorubicin downregulates vimentin and aggresome-promoting factors

To investigate the mechanism through which doxorubicin inhibits bortezomib-induced aggresome formation, we examined various aggresome-promoting factors, including the structural protein Vimentin and several misfolded protein recognition or transport factors. These included HDAC6 and its upstream transcriptional regulator c-Myc, p62 and its upstream transcriptional regulator

NRF2 and activator p38, HSP70, BAG3, and 14-3-3 proteins, eEF1A1, HOOK2, and Dynein with its associated subunits. Furthermore, we examined aggresome or misfolded protein clearance-related factors such as HSP90 and autophagy-promoting factors like LC3 and ATG4C since autophagosomes are primarily responsible for aggresome clearance. Our results demonstrated that doxorubicin significantly downregulated the protein levels of aggresome structural and promoting factors in bortezomib-treated cells. These included Vimentin, HDAC6, the NRF2-p62 axis, phosphorylated p38, 14-3-3 η , 14-3-3 ζ , eEF1A1, HOOK2, and Dynein along with its subunits DYNLL1 and DNAH5 (Fig. 3). However, key regulators of misfolded protein clearance or autophagosome formation, such as HSP90, LC3, and ATG4C, remained unaffected by doxorubicin in bortezomib-treated cells.

Cotreatment with doxorubicin and bortezomib increased accumulation of misfolded proteins and amplified ER or Golgi stress responses as well as apoptosis/necroptosis in U266B1 cells

Proteasome inhibitors eliminate cancer cells by accumulating misfolded proteins. We first examined these misfolded protein toxicants and found that cotreatment

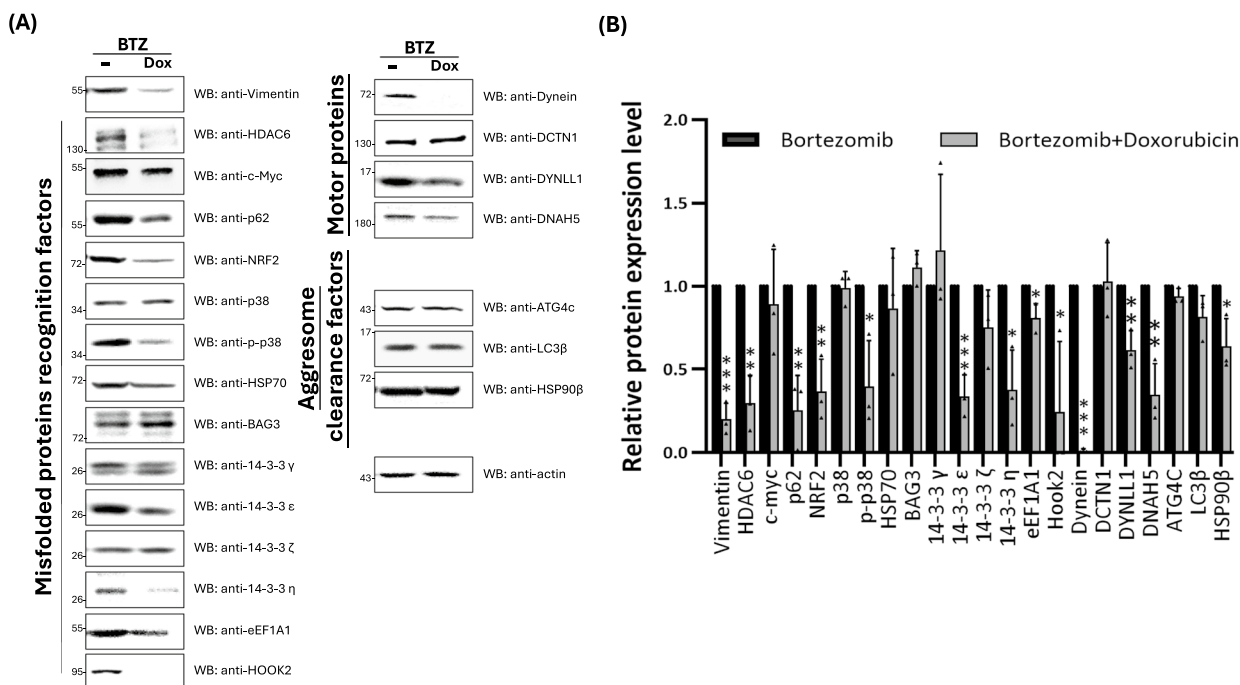


Fig. 3 Doxorubicin downregulates Vimentin and various aggresome-promoting factors. U266B1 cells were treated with 6.25 nM bortezomib or a combination of 6.25 nM bortezomib and 1 μM doxorubicin, followed by Western blot analysis to assess the protein levels of key aggresome components, including Vimentin (a structural component of the aggresome), aggresome-promoting factors such as misfolded protein recognition proteins, motor proteins involved in misfolded protein transport, and aggresome clearance factors (A). The relative protein levels were quantified and plotted, with statistical significance indicated (B). Statistical significance was determined using t-tests, with *p < 0.05, **p < 0.01, and ***p < 0.001. All experiments were performed independently three times

of doxorubicin and bortezomib increased the levels of ubiquitinated misfolded proteins (Fig. 4A). It is known that bortezomib induces cell death by triggering ER stress [19]. Furthermore, Golgi-disrupting agents like Brefeldin A, can cause a Golgi stress response [20], and the Golgi apparatus undergoes structural fragmentation during aggresome formation or proteasome inhibitor treatment [21], suggesting that Golgi stress may also contribute to bortezomib-induced cell death.

Accordingly, we examined factors involved in the ER or Golgi stress responses. Our findings revealed that the protein levels of proapoptotic factors associated with ER stress, such as CHOP, ATF3, and ATF4, and those involved in Golgi stress, including ARF4, CREB3, and ETS1/2, were elevated when doxorubicin was added to bortezomib-treated U266B1 cells (Fig. 4B, C), although the prosurvival factor HSP47 in the Golgi stress response was also increased. Since sustained ER or Golgi stress often leads to cell death by inducing apoptosis, we examined the expression of proapoptotic factors and multiple caspases (Fig. 4D, E). The results revealed a significant increase in Bad, Bik, Bim, BID, Bak, and Puma levels, along with activated Caspases 3, 7, 9, and PARP, in U266B1 cells treated with bortezomib and doxorubicin.

Lastly, ER stress has also been implicated in inducing necroptosis [22], and our results showed that RIPK1, a key factor in necroptosis, was elevated in cells cotreated with bortezomib and doxorubicin compared with bortezomib alone (Fig. 4F). In summary, our analyses revealed that doxorubicin enhanced bortezomib-induced cell death by increasing the accumulation of misfolded proteins and exacerbating ER and Golgi stress responses, consequently leading to a stronger induction of apoptosis and necroptosis.

Doxorubicin did not synergize cell mortality induced by proteasome inhibitors lacking aggresome-inducing activity

Capzimin and clioquinol are two proteasome inhibitors that function through different mechanisms: Capzimin inhibits the isopeptidase activity of the proteasomal subunit RPN11 [23], while clioquinol acts as an ionophore, directing metal ions to disrupt the proteasomal enzymatic complex [24]. Notably, neither of these proteasome inhibitors can induce aggresome formation. Despite that the cells underwent capzimin treatment, Vimentin networks reorganized into a cage-like structure; however, no ubiquitinated aggregates were observed within the cage (Fig. 5A). To verify this, we also examined HDAC6 localization, a key protein in misfolded protein recognition and transport. Unlike bortezomib, which stimulates the recruitment of HDAC6 and ubiquitin to aggresomes, capzimin failed to induce the accumulation of either HDAC6 or ubiquitin in treated cells (Fig. 5B). Furthermore, at doses that induced 30–40% cell death, capzimin did not synergize with doxorubicin to enhance cell mortality (Fig. 5C). Similarly, clioquinol treatment failed to induce Vimentin cage formation or ubiquitin aggregation (Fig. 5D), and no synergistic increase in cell death was observed when clioquinol was combined with doxorubicin (Fig. 5E). These findings suggest that the ability of proteasome inhibitors to induce aggresome formation is crucial for their synergy with doxorubicin in promoting cell death.

(See figure on next page.)

Fig. 4 Cotreatment with doxorubicin increases misfolded protein accumulation, enhances ER/Golgi stress responses and promotes apoptosis/necroptosis in bortezomib-treated cells. **A** Cotreatment with doxorubicin increases the level of ubiquitinated proteins in bortezomib-treated cells. U266B1 cells exposed to bortezomib or the combination of bortezomib and doxorubicin were analyzed for misfolded protein levels by Western blot using anti-ubiquitin antibodies. The relative protein levels were quantified and plotted with statistical significance. **B** Cotreatment with doxorubicin elevates the protein levels of factors that promote ER stress-dependent apoptosis in bortezomib-treated cells. U266B1 cells exposed to bortezomib or the combination were analyzed by Western blot for the levels of ER stress response regulators, including IRE1, pIRE-S724, GRP78, CHOP, ATF3, and ATF4. The relative protein levels were plotted with statistical significance. **C** Cotreatment with doxorubicin increases the protein levels of factors involved in Golgi stress-dependent apoptosis in bortezomib-treated cells. Western blot analysis was performed on U266B1 cells treated with bortezomib or the combination, focusing on Golgi stress response regulators such as ARF4, CREB3, ETS1, ETS2, and HSP47. The relative protein levels were quantified and plotted. **D** Cotreatment with doxorubicin enhances the levels of proapoptotic factors in Bortezomib-treated cells. U266B1 cells were analyzed by Western blot for proapoptotic factors such as Bad, pBad (S112), Bax, Bik, Bim, BID, Bak, and Puma. The relative protein levels were plotted with statistical significance. **E** Cotreatment with doxorubicin increases the levels of active caspases in bortezomib-treated cells. Western blot analysis was performed on U266B1 cells exposed to Bortezomib or the combination, measuring the levels of the proform and cleaved active forms of caspases 3, 6, 7, 9, and PARP. The relative protein levels were plotted with statistical significance. **F** Cotreatment with doxorubicin elevates the protein level of RIPK1, a key factor promoting necroptosis, in Bortezomib-treated cells. U266B1 cells were analyzed by Western blot for necroptosis regulators, including RIPK1, RIPK2, and RIPK3. The relative protein levels were quantified and plotted with statistical significance. Statistical significance was determined using t-tests, with * $p < 0.05$, ** $p < 0.01$, and *** $p < 0.001$. All experiments were performed independently three times

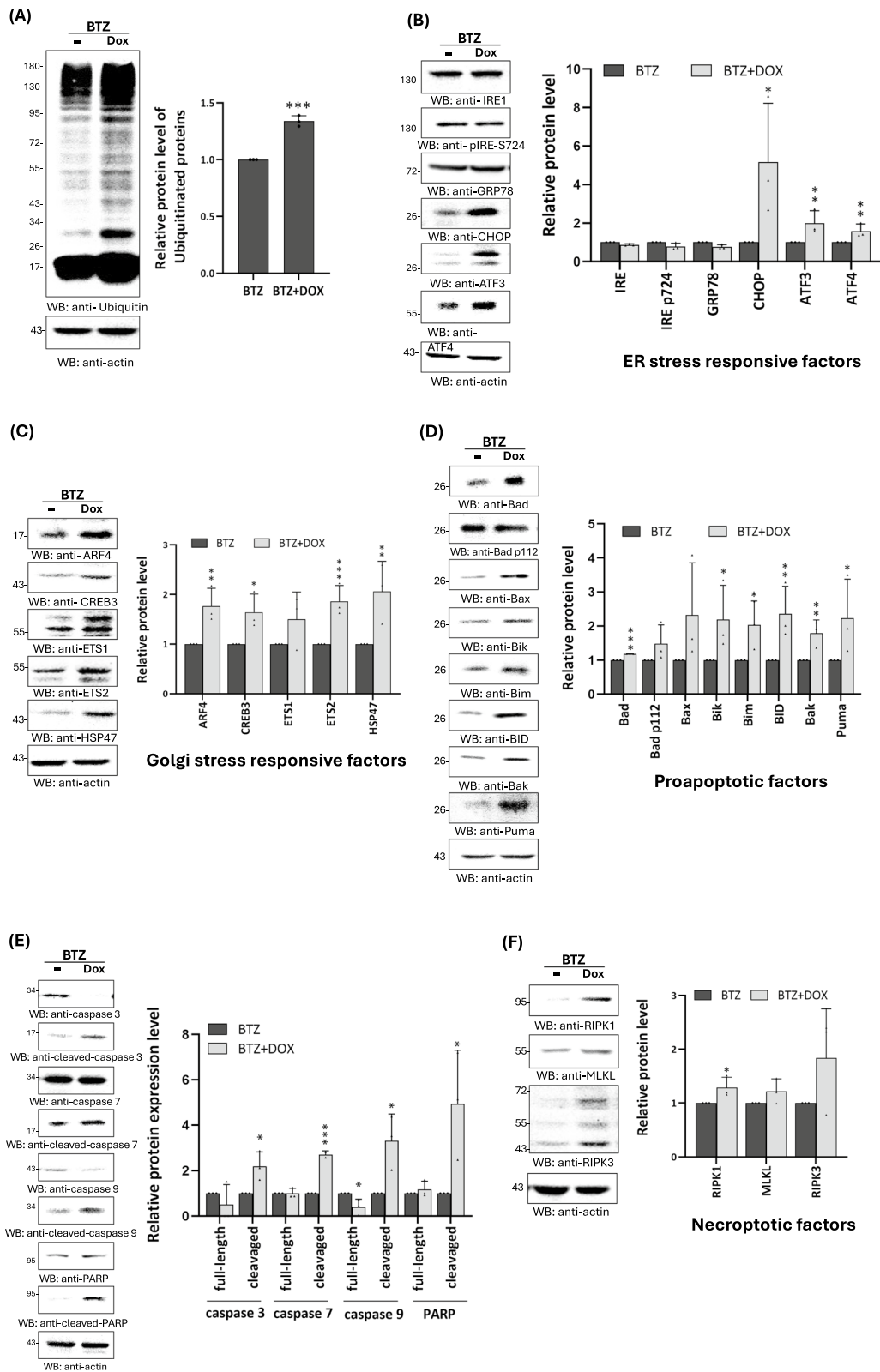


Fig. 4 (See legend on previous page.)

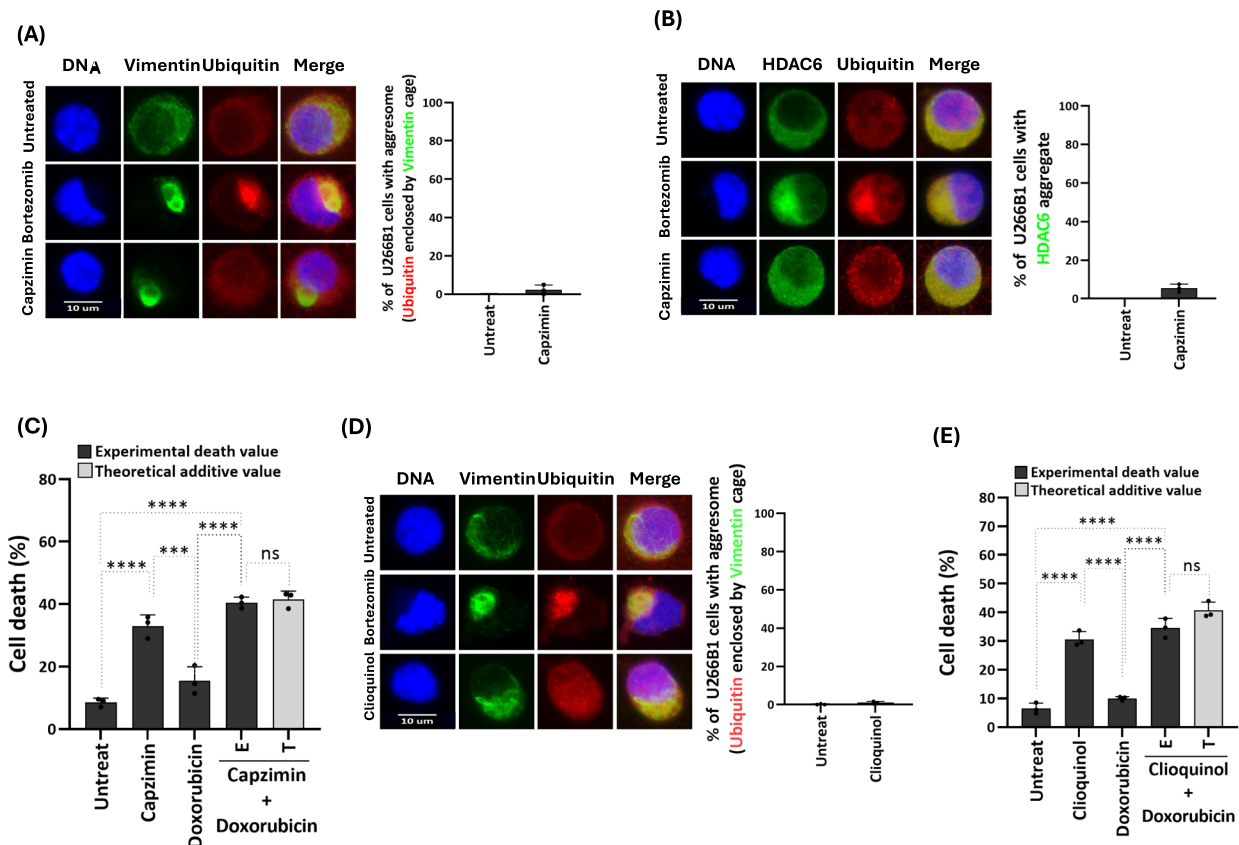


Fig. 5 Doxorubicin does not synergize with cell mortality triggered by proteasome inhibitors lacking aggresome-inducing activity. **A** Capzimin does not stimulate aggresome formation. U266B1 cells treated with no compound or 5 μ M Capzimin for 24 h, which resulted in ~ 30% cell death, were analyzed for aggresome formation using immunofluorescence. The percentage of cells with aggresomes (Ubiquitin aggregates enclosed by Vimentin cages, as defined previously) was counted and plotted. 6.25 nM bortezomib was used as a positive control. **B** Confirmation of Capzimin's inability to stimulate aggresome formation. U266B1 cells treated with no compound or 5 μ M Capzimin for 24 h were analyzed by immunofluorescence using antibodies against Ubiquitin and HDAC6, which is responsible for recognizing and transporting misfolded proteins to the aggresome. The percentage of Capzimin-treated cells with HDAC6 aggregates was counted and plotted. 6.25 nM Bortezomib was used as a positive control, where Ubiquitin and HDAC6 colocalized, confirming HDAC6's role in recognizing and binding ubiquitinated misfolded proteins. **C** Capzimin does not synergize with Doxorubicin to enhance cell death. U266B1 cells treated with no chemical, 5 μ M Capzimin, or Capzimin plus 1 μ M doxorubicin for 24 h were analyzed for cell death using the trypan blue exclusion assay. The experimental death value (E) represents the observed cell death from the combined treatment, whereas the theoretical additive value (T) represents the sum of cell death induced by each drug alone. **D** Clioquinol does not stimulate aggresome formation. U266B1 cells treated with no compound, 6.25 nM bortezomib, or 25 μ M Clioquinol for 24 h, which resulted in ~ 30% cell death, were analyzed for aggresome formation by immunofluorescence. The percentage of cells with aggresomes was counted and plotted. **E** Clioquinol does not synergize with Doxorubicin to enhance cell death. U266B1 cells treated with no chemical, 25 μ M Clioquinol, or Clioquinol plus 1 μ M doxorubicin for 24 h were analyzed for cell death using the trypan blue exclusion assay. The experimental death value (E) represents the observed cell death from the combined treatment, whereas the theoretical additive value (T) represents the sum of cell death induced by each drug alone. *** and **** indicate statistical significance based on one-way ANOVA with Tukey's multiple comparison test with $p < 0.001$ and $p < 0.0001$, respectively. Ns indicates no significance. All experiments were performed independently three times. Scale bar: 10 μ m

Doxorubicin did not synergize bortezomib-induced cell death in multiple myeloma cell lines that lack aggresome-forming activity

Furthermore, we evaluated the cell-killing effects of bortezomib and doxorubicin in RPMI-8226 and NCI-H929 MM cell lines. Unlike U266B1, these two cell lines did not develop aggresomes in response to bortezomib treatment (Fig. 6A). In these cell lines, Vimentin

either displayed no signal or showed disorganized patterns, and ubiquitin appeared as dispersed or multiple separated aggregates. Moreover, RPMI-8226 and NCI-H929 cells exhibited very low levels of Vimentin and HDAC6 (Fig. 6B). Vimentin forms the structural framework of aggresomes, whereas HDAC6 is involved in recognizing misfolded proteins and utilizing Dynein to transport ubiquitinated misfolded proteins to

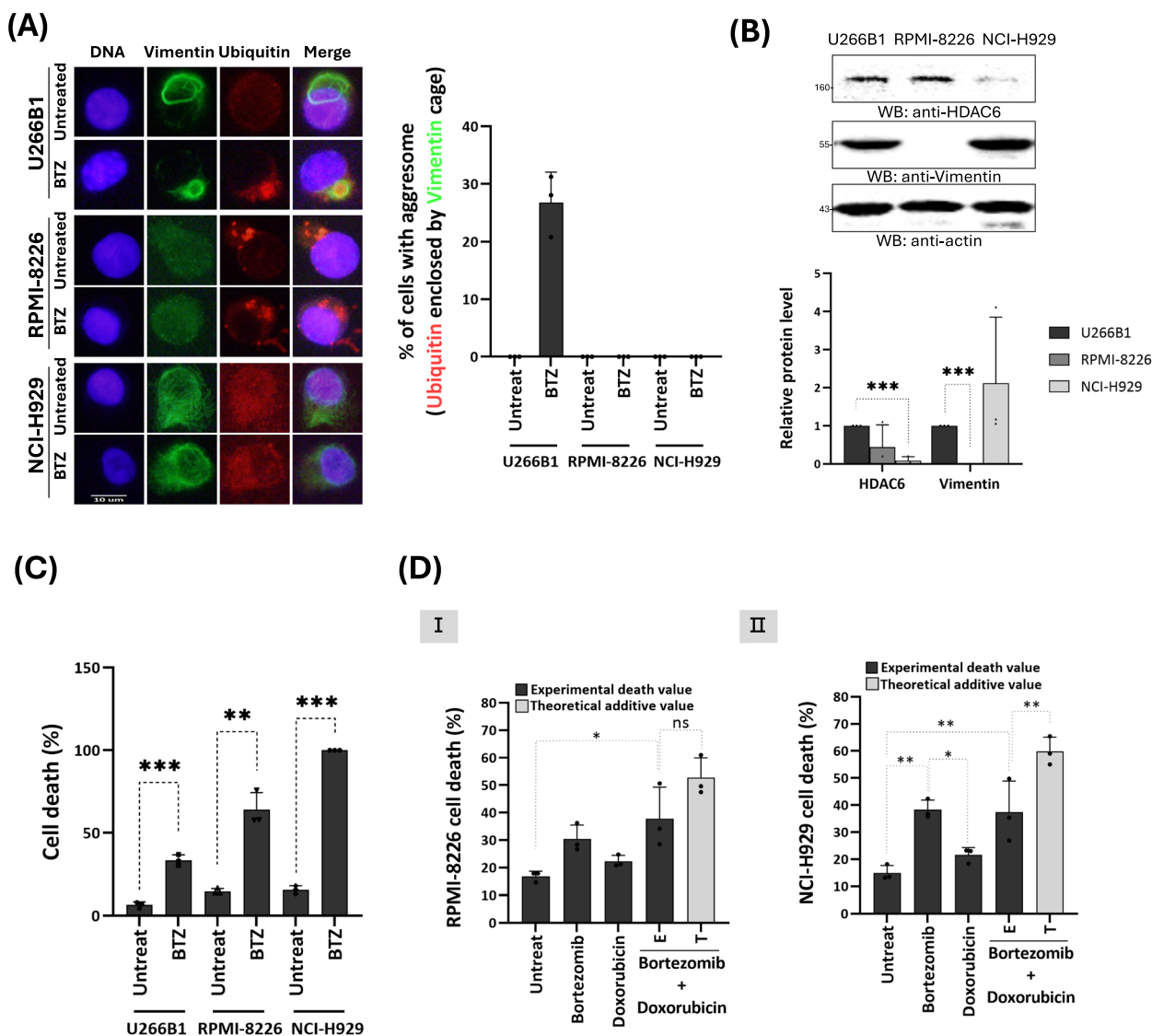


Fig. 6 Doxorubicin does not synergize with bortezomib-induced cell mortality in multiple myeloma (MM) cells lacking aggresome-forming activity. **A** Aggresome formation status in several MM cell lines. U266B1, RPMI-8226, and NCI-H929 cells were treated with 6.25 nM bortezomib (U266B1 and RPMI-8226) or 1.5 nM Bortezomib (NCI-H929) for 18 h. The lower bortezomib dose in NCI-H929 cells was used owing to the high sensitivity of these cells to 6.25 nM bortezomib. Immunofluorescence was performed to detect aggresome formation, and the percentage of cells with Ubiquitin aggregates enclosed by a Vimentin cage was quantified and plotted. **B** Differential expression of Vimentin and HDAC6 in the three MM cell lines. U266B1, RPMI-8226, and NCI-H929 cells were analyzed by Western blot to determine the protein levels of Vimentin and HDAC6. The relative protein levels were quantified and plotted with statistical significance. **C** Differential sensitivity of the three cell lines to bortezomib. U266B1, RPMI-8226, and NCI-H929 cells were treated with 6.25 nM bortezomib for 24 h, and cell mortality was determined using the trypan blue exclusion assay. **D** Combined treatment with bortezomib and doxorubicin did not produce synergistic cell death in RPMI-8226 or NCI-H929 cells. RPMI-8226 (I) and NCI-H929 (II) cells were treated with 2.5 nM and 1.5 nM bortezomib, respectively, 0.5 μM and 0.25 μM doxorubicin, or the combination for 24 h, followed by an analysis of cell death using the trypan blue exclusion assay. Under these conditions, ~40% cell mortality was observed with bortezomib and ~20% with doxorubicin in both cell lines. The experimental death value (E) represents the observed cell death induced by the combined treatment, whereas the theoretical additive value (T) represents the sum of the cell death induced by each drug alone. Statistical analysis: **B** and **C** were analyzed using a t-test with ** $p < 0.01$ and *** $p < 0.001$; (D) was analyzed using one-way ANOVA with Tukey's multiple comparison test, with * $p < 0.05$ and ** $p < 0.01$. ns indicates no significance. All experiments were performed independently three times. Scale bar: 10 μm

aggresomes. These findings collectively explained the low aggresome-forming activity in RPMI-8226 and NCI-H929 cells.

Interestingly, RPMI-8226 and NCI-H929 cells exhibited a higher death rate compared to U266B1 cells when treated with bortezomib (Fig. 6C), supporting the notion that aggresomes play a cytoprotective role against proteasome inhibitor-induced accumulation of toxic misfolded proteins. Since our results identified doxorubicin as an aggresome-blocking agent, we further investigated whether its ability to potentiate bortezomib-induced cell death was lost in RPMI-8226 and NCI-H929 cells, which exhibit minimal aggresome-forming activity. Indeed, no synergistic cell death was observed in RPMI-8226 and NCI-H929 cells treated with bortezomib and doxorubicin (Fig. 6D).

Autophagy inhibitors did not enhance the drug synergy of bortezomib and doxorubicin in inducing cell mortality

To further enhance the drug synergy of the combined treatment of bortezomib and doxorubicin, autophagy inhibitors were tested based on reports that misfolded proteins sequestered by aggresomes are cleared through autophagosomes [25]. Four autophagy inhibitors were examined: 3-MA and vps34-PIK-III, which block autophagy by inhibiting phosphatidylinositol 3-kinase; and chloroquine and MHY1485, which impair the fusion of autophagosomes with lysosomes. The results revealed that chloroquine maintained the bortezomib-doxorubicin synergy in cell death, whereas the other three inhibitors abolished it (Fig. 7A–D). Notably, chloroquine alone synergized with bortezomib to increase cell death (Fig. 7C). Further analysis revealed that chloroquine blocked bortezomib-induced aggresome formation but did not further enhance doxorubicin's inhibition of aggresome formation (Fig. 7E). This finding aligns with the observation that chloroquine did not improve the drug synergy in cell death induced by the combination of bortezomib and doxorubicin (Fig. 7C).

Discussion

This study demonstrated that doxorubicin significantly enhanced bortezomib-induced cytotoxicity and disrupted aggresome formation in MM U266B1 cells. Mechanistic analysis revealed that doxorubicin downregulated key aggresome components and regulatory factors, including Vimentin, HDAC6, and Dynein, while also exacerbating ER and Golgi stress responses, thereby further activating pro-apoptotic or necroptotic pathways in bortezomib-treated MM cells. Notably, doxorubicin failed to potentiate cell death induced by proteasome inhibitors that did not stimulate aggresome formation. Furthermore, the combination of bortezomib and doxorubicin failed to produce synergistic cell death in MM cells, which lacked aggresome formation capability.

This study evaluated several compounds for their potential to enhance bortezomib-induced cell death in MM cells. Established anti-MM drugs, including doxorubicin, lenalidomide, pomalidomide, and dexamethasone, were tested alongside experimental agents such as alisertib, regorafenib, gemcitabine, EPZ015666, and doxorubicin were found to inhibit MG132-induced aggresome formation and synergize MG132-mediated cell death in A549 lung cancer cells (Supplementary Fig. 1). However, co-treatment of bortezomib with lenalidomide, pomalidomide, dexamethasone, alisertib, or regorafenib failed to achieve additive cell death in MM cells. These findings highlight the challenges in achieving drug synergy with bortezomib in U266B1 MM cells and emphasize the need for novel, more effective anti-MM treatment regimens.

Our results demonstrated that doxorubicin synergized with bortezomib to induce MM cell death by inhibiting aggresome formation and triggering ER/Golgi stress and apoptosis. Doxorubicin, a versatile anticancer agent with multiple mechanisms of action [26], was first identified in our study as an aggresome-blocking agent, achieved by downregulating key structural components of the aggresome, including Vimentin, misfolded protein recognition factors such as HDAC6, eEF1A1, and p62, as well as the transport motor Dynein and its subunits DYNLL1 and DNAH5. Several lines of evidence support our conclusion that doxorubicin potentiated

(See figure on next page.)

Fig. 7 Autophagy inhibitors do not further enhance the drug synergy between bortezomib and doxorubicin. **A–D** U266B1 cells were treated with either no compound, 6.25 nM bortezomib, 1 μ M doxorubicin, or one of the following autophagy inhibitors: 2 mM 3-MA (**A**), 1 μ M Vps34-PIK-III (**B**), 20 μ M Chloroquine (**C**), or 2.5 μ M MHY1485 (**D**), or combinations of two or three compounds. After 24 h, trypan blue exclusion assays were performed to assess cell death. The experimental death value (E) represents the observed cell death induced by the combined treatment, whereas the theoretical additive value (T) represents the sum of cell death induced by each drug individually. **E** Chloroquine inhibits bortezomib-induced aggresome formation but does not further enhance doxorubicin-mediated inhibition of aggresome formation. U266B1 cells treated with no compound, 6.25 nM Bortezomib, 1 μ M Doxorubicin, 20 μ M Chloroquine, or combinations of two or three compounds were analyzed for aggresome formation. The percentage of cells with aggresomes was counted and plotted. Statistical significance was determined by t-tests, with * $p < 0.05$, ** $p < 0.01$, and *** $p < 0.001$. All experiments were performed independently three times. Scale bar: 10 μ m

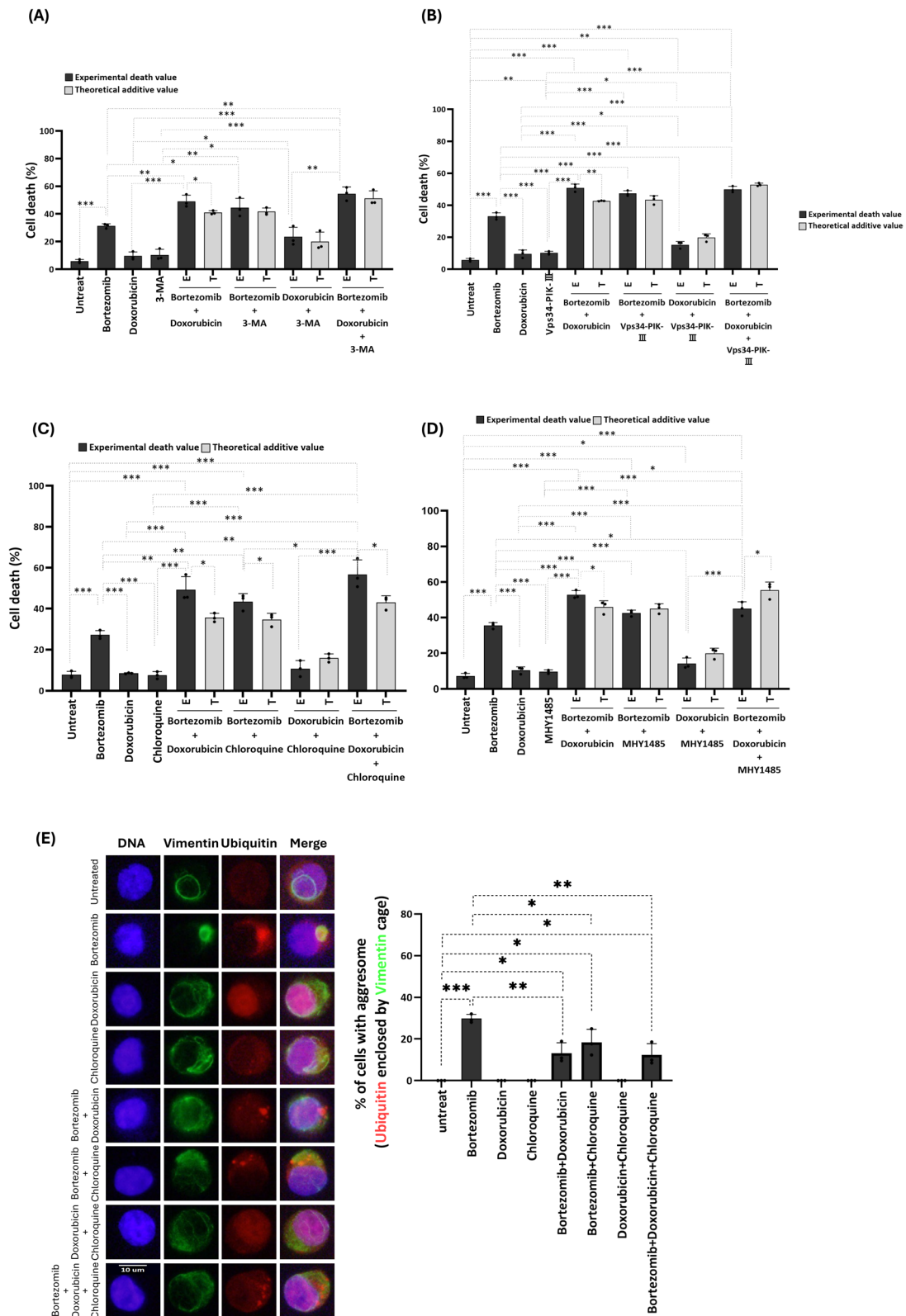


Fig. 7 (See legend on previous page.)

bortezomib-induced cell death by disrupting aggresome formation, leading to ER/Golgi stress and apoptosis/necroptosis.

First, doxorubicin only synergized with agents capable of inducing aggresome formation, such as bortezomib. In contrast, proteasome inhibitors capzimin and the proteasome-inhibiting compound clioquinol failed to induce aggresome formation and failed to enhance doxorubicin's cytotoxicity. Interestingly, the autophagy inhibitor chloroquine, which blocked aggresome formation, synergized with doxorubicin to induce MM cell death. Furthermore, the combination of bortezomib and doxorubicin did not produce synergistic cell death in RPMI-8226 and NCI-H929 MM cell lines, which lacked aggresome-forming capacity. The rationale behind the observed synergy was that doxorubicin, as an aggresome inhibitor, disrupted aggresome formation, releasing misfolded proteins into the cytoplasm, which enhanced bortezomib-induced MM cell death. In cases where aggresome formation was absent—whether owing to treatment with capzimin, clioquinol, or in the RPMI-8226 and NCI-H929 cell lines—doxorubicin had no opportunity to enhance bortezomib-induced cytotoxicity.

Secondly, the co-treatment with bortezomib and doxorubicin further increased the accumulation of ubiquitinated misfolded proteins in the cytoplasm.

Typically, these toxic misfolded proteins are sequestered and degraded through the aggresome-autophagy pathway. However, by disrupting aggresome formation, doxorubicin forced these protein toxicants into the cytoplasm. Thirdly, several factors involved in the ER or Golgi stress response, along with pro-apoptotic factors, caspases, and pro-necroptotic factors, were upregulated by the co-treatment with bortezomib and doxorubicin. This suggests that, without aggresome-mediated sequestration, misfolded proteins more actively damage subcellular structures, leading to the augmentation of ER/Golgi stress, and subsequently, apoptosis/necroptosis.

Autophagosomes are known to help clear misfolded proteins within the aggresome. However, surprisingly, co-treatment with autophagy inhibitors failed to sustain the bortezomib-doxorubicin-induced synergy in MM cell death. This observation could be owing to the fact that proteasome activity is required for the activation of autophagy [27], leading to the ongoing debate on whether autophagy alleviates proteotoxic stress in proteasome-inhibited cells [28]. Furthermore, proteasome washout experiments also revealed that aggresome-associated ubiquitinated proteins were efficiently degraded through autophagy once proteasome resumed activity [29]. Our findings further indicated that co-treatment with autophagy inhibitors, except chloroquine, diminished the synergy between bortezomib and doxorubicin.

These imply that autophagy played a minor role in degrading misfolded proteins sequestered by aggresome. Instead, other degradation pathways were responsible for clearing these proteins, leading to the accumulation of ubiquitinated misfolded proteins in cells co-treated with bortezomib and doxorubicin. Notably, only chloroquine maintained the drug synergy with bortezomib and doxorubicin without further enhancing it. Interestingly, chloroquine blocked aggresome formation and synergistically enhanced doxorubicin-induced U266B1 MM cell death, further confirming that the proteasome inhibitor with aggresome-inducing activity can synergize with doxorubicin in mediating cell death.

Clinically, bortezomib plays a crucial role in the treatment of newly diagnosed MM [30]. However, cells exposed to bortezomib can develop aggresome, leading to eventual drug resistance. To enhance therapeutic efficacy against MM, our study suggested that combining bortezomib, at a dose with moderate cytotoxicity and significant aggresome-promoting activity, with doxorubicin at a low-cytotoxicity dose resulted in synergistic cell death in U266B1 MM cells. The ratio of the experimental death value to the theoretical additive value (E/T ratio) averaged 1.2 across five results, as shown in Figs. 1A, 6A–D. Therefore, a low-toxicity dose of doxorubicin could significantly enhance the bortezomib-mediated cell mortality rate, achieving a synergistic cell death rate 1.2 times higher than the expected additive toxicity of both drugs. Notably, most other anticancer agents in our study failed to reach additive toxicity with bortezomib. This combination, targeting MM cells misfolded protein-productions, showed promise in overcoming aggresome-mediated resistance to bortezomib. A Phase III randomized trial by Orłowski et al. [31] demonstrated that the combination of pegylated liposomal doxorubicin with bortezomib extended the time to progression in relapsed and refractory MM compared with bortezomib alone. Our study provides possible mechanistic insights into how the multidrug regimen functions in MM cells. Although further evidence is needed, the percentage of clonal plasma cells with aggresome formation could potentially serve as a biomarker for predicting the efficacy of doxorubicin and bortezomib combination therapy in treating relapsed and refractory MM.

The lack of *in vivo* mouse model represents a significant limitation of this study. However, the primary focus of this research is on mechanism-based analyses at the cellular and organelle levels, proposing the aggresome as the drug target of doxorubicin to enhance bortezomib-induced cell mortality. The varying proliferation rates of different MM cell lines, with or without aggresome-forming activity, could introduce confounding variables when evaluating aggresome-dependent

drug effects in a mouse model. This challenge is further compounded by the need for co-treatment with doxorubicin and bortezomib. Nonetheless, we are actively considering the development of a mouse model to complement our findings and plan to strengthen our conclusions with an *in vivo* approach in the future.

Conclusion

We demonstrated that doxorubicin inhibits bortezomib-induced aggresome formation while enhancing bortezomib-induced cell death. Mechanistic studies revealed that doxorubicin downregulates key aggresome-promoting factors and amplifies pro-apoptotic or necroptotic pathways by intensifying ER and Golgi stress responses in bortezomib-treated MM cells. Notably, the inability of doxorubicin to synergize with cell death induced by proteasome inhibitors that do not stimulate aggresome formation or in cell lines lacking aggresome-forming activity suggests that doxorubicin specifically enhances bortezomib-induced cytotoxicity by inhibiting aggresome formation.

Abbreviations

MM	Multiple myeloma
HDAC6	Histone deacetylase 6
ER	Endoplasmic reticulum
HSP70	Heat Shock Protein 70
BAG3	Bcl-2-associated athanogene 3
eEF1A1	Eukaryotic Elongation Factor 1 Alpha 1
1 DCTN1	Dynactin Subunit
RPMI	Roswell Park Memorial Institute
3-MA	3-Methyladenine
Vps34-PIK III	Vacuolar protein sorting 34-phosphatidylinositol 3-kinase III
c-Myc	Cellular myelocytomatosis
NRF2	Nuclear factor erythroid 2-related factor 2
HOOK2	Hook microtubule-tethering protein 2
DYNLL1	Dynein light chain LC8-type 1
DNAH5	Dynein axonemal heavy chain 5
ATG4C	Autophagy-related 4C cysteine peptidase
IRE1	Inositol-requiring enzyme 1
pIRE S724	Phosphorylated IRE1 serine
GRP78	Glucose-regulated protein 78
CHOP	C/EBP homologous protein
ATF3	Activating transcription factor 3
ARF4	ADP-ribosylation factor 4
CREB3	Cyclic AMP-responsive element-binding protein 3
ETS1	E26 transformation-specific sequence 1
Bad	Bcl-2-associated death promoter
Bax	Bcl-2-associated X protein
Bik	Bcl-2-interacting killer
Bim	Bcl-2-interacting mediator of cell death
BID	BH3-interacting domain death agonist
Bak	Bcl-2 homologous antagonist/killer
Puma	P53 upregulated modulator of apoptosis
PARP	Poly(ADP-ribose) polymerase
RIPK1	Receptor-interacting serine/threonine-protein kinase 1
HRP	Horse radish peroxidase
EDTA	Ethylenediaminetetraacetic acid
PVDF	Polyvinylidene difluoride
TBST	Tween 20

Supplementary Information

The online version contains supplementary material available at <https://doi.org/10.1186/s12967-024-05920-2>.

Supplementary Material. Supplemental Fig. 1. Effects of Alisertib, Regorafenib, Gemcitabine, EPZ015666, and Doxorubicin on the inhibition of aggresome formation and enhancement of MG132-induced cell death in A549 cells. A549 cells were treated with either no compound, 5 μ M MG132, or one of the following: 5 or 10 μ M Alisertib (A, B), 10 or 25 μ M Regorafenib (C, D), 50 μ M EPZ015666 (E, F), 6.25 or 12.5 μ g/ml Gemcitabine (G, H), or 5 μ M doxorubicin (I, J), either alone or in combination with MG132. After 24 h, cell death was assessed microscopically, with particular attention to markers such as membrane blebbing. The experimental death value (E) represents the observed cell death resulting from the combined drug treatments, whereas the theoretical additive value (T) reflects the sum of the cell death induced by each drug individually. Statistical analysis: (A), (C), (E), (G)—t-test, * $p < 0.05$, ** $p < 0.01$, *** $p < 0.001$; (B), (D), (F), (H)—one-way ANOVA with Tukey's multiple comparison test, * $p < 0.05$, ** $p < 0.01$, *** $p < 0.001$, **** $p < 0.0001$.

Author contributions

Chang-Tze Ricky Yu: Conceptualization, investigation, formal analysis, writing—review and editing. Yu-Ting Amber Liao, Chi-Yin Nina Chiang, Jo-Mei Maureen Chen: Investigation, formal analysis, writing—review and editing. Hsin-Yu Bella Pan, Chia-Yun Pan, Wei-Jun Jiang, Jia-Rung Tsai, Tsung-Ying Yang: Methodology, investigation, writing—review and editing. Chieh-Lin Jerry Teng: Conceptualization, supervision, writing—review and editing. All authors gave final approval of the manuscript.

Funding

The present study was funded by Taichung Veterans General Hospital (TCVGH-1133701C), Taichung Veterans General Hospital/Show Chwan Care System Joint Research Program (TCVGH-SCCS-SRD113005), National Science and Technology Council (NSTC 113-2320-B-260 -001 -MY3), and Taichung Veterans General Hospital-National Chi Nan university Joint Research Program (TCVGH-NCNU1127903, TCVGH-NCNU1137903).

Data availability

The datasets used and/or analyzed during the current study are available from the corresponding author on reasonable request.

Declarations

Ethics approval and consent to participate

Not applicable.

Consent for publication

Not applicable.

Competing interests

Chieh-Lin Jerry Teng received honorarium and consulting fees from Novartis, Roche, Pfizer, Takeda, Johnson and Johnson, Amgen, BMS Celgene, Kirin, TTY, and MSD. The other authors have no conflicts of interest.

Author details

¹Department of Applied Chemistry, National Chi Nan University, No. 1 University Rd., Puli Township, Nantou 545301, Taiwan. ²Division of Hematology/Medical Oncology, Department of Medicine, Taichung Veterans General Hospital, No. 1650 Taiwan Boulevard, Sect. 4, Taichung 407219, Taiwan. ³Department of Chest Medicine, Taichung Veterans General Hospital, No. 1650 Taiwan Boulevard, Sect. 4, Taichung 407219, Taiwan. ⁴Department of Life Sciences, National Chung Hsing University, No. 145 Xingda Rd., South Dist., Taichung 402202, Taiwan. ⁵Department of Post-Baccalaureate Medicine, College of Medicine, National Chung Hsing University, No. 145 Xingda Rd., South Dist., Taichung 402202, Taiwan. ⁶Ph.D. Program in Translational Medicine, National Chung Hsing University, No. 145 Xingda Rd., South Dist., Taichung 402202, Taiwan. ⁷Rong Hsing Research Center for Translational Medicine, National Chung Hsing University, No. 145 Xingda Rd., South Dist., Taichung 402202, Taiwan.

⁸School of Medicine, Chung Shan Medical University, No. 110, Sect. 1, Jianguo North Rd., Taichung 40201, Taiwan. ⁹Department of Life Science, Tunghai University, No. 1727 Taiwan Boulevard, Sect. 4, Taichung 407224, Taiwan.

Received: 14 September 2024 Accepted: 26 November 2024
Published online: 03 December 2024

References

- Gomes CM. Protein misfolding in disease and small molecule therapies. *Curr Top Med Chem.* 2012;12(22):2460–9.
- Winklhofer KF, Tatzelt J, Haass C. The two faces of protein misfolding: gain- and loss-of-function in neurodegenerative diseases. *EMBO J.* 2008;27(2):336–49.
- Coyne LP, Chen XJ. Consequences of inner mitochondrial membrane protein misfolding. *Mitochondrion.* 2019;49:46–55.
- Cheng B, Li Y, Ma L, Wang Z, Petersen RB, Zheng L, et al. Interaction between amyloidogenic proteins and biomembranes in protein misfolding diseases: mechanisms, contributors, and therapy. *Biochim Biophys Acta Biomembr.* 2018;1860(9):1876–88.
- Liang G, Lian C, Huang D, Gao W, Liang A, Peng Y, et al. Endoplasmic reticulum stress-unfolding protein response-apoptosis cascade causes chondrodysplasia in a col2a1 pGly1170Ser mutated mouse model. *PLoS ONE.* 2014;9(1): e86894.
- Fricker LD. Proteasome inhibitor drugs. *Annu Rev Pharmacol Toxicol.* 2020;60:457–76.
- Kawaguchi Y, Kovacs JJ, McLaurin A, Vance JM, Ito A, Yao TP. The deacetylase HDAC6 regulates aggresome formation and cell viability in response to misfolded protein stress. *Cell.* 2003;115(6):727–38.
- Jia B, Wu Y, Zhou Y. 14-3-3 and aggresome formation: implications in neurodegenerative diseases. *Prion.* 2014;8(2):173–7.
- Park Y, Park J, Kim YK. Crosstalk between translation and the aggresome-autophagy pathway. *Autophagy.* 2018;14(6):1079–81.
- Nassar M, Samaha H, Ghabriel M, Yehia M, Taha H, Salem S, et al. LC3A silencing hinders aggresome vimentin cage clearance in primary choroid plexus carcinoma. *Sci Rep.* 2017;7(1):8022.
- Hideshima T, Bradner JE, Wong J, Chauhan D, Richardson P, Schreiber SL, et al. Small-molecule inhibition of proteasome and aggresome function induces synergistic antitumor activity in multiple myeloma. *Proc Natl Acad Sci USA.* 2005;102(24):8567–72.
- Lee SW, Yeon SK, Kim GW, Lee DH, Jeon YH, Yoo J, et al. HDAC6-selective inhibitor overcomes bortezomib resistance in multiple myeloma. *Int J Mol Sci.* 2021;22(3):1341.
- van de Donk N, Pawlyn C, Yong KL. Multiple myeloma. *Lancet.* 2021;397(10272):410–27.
- Attal M, Lauwers-Cances V, Hulin C, Leleu X, Caillot D, Escoffre M, et al. Lenalidomide, bortezomib, and dexamethasone with transplantation for myeloma. *N Engl J Med.* 2017;376(14):1311–20.
- Adams J, Behnke M, Chen S, Cruickshank AA, Dick LR, Grenier L, et al. Potent and selective inhibitors of the proteasome: dipeptidyl boronic acids. *Bioorg Med Chem Lett.* 1998;8(4):333–8.
- Terpos E, Roussou M, Dimopoulos MA. Bortezomib in multiple myeloma. *Expert Opin Drug Metab Toxicol.* 2008;4(5):639–54.
- Kozalak G, Butun I, Toyran E, Kosar A. Review on bortezomib resistance in multiple myeloma and potential role of emerging technologies. *Pharmaceuticals.* 2023;16(1):111.
- Lehar J, Krueger AS, Avery W, Heilbut AM, Johansen LM, Price ER, et al. Synergistic drug combinations tend to improve therapeutically relevant selectivity. *Nat Biotechnol.* 2009;27(7):659–66.
- Zhang Y, Bai C, Lu D, Wu X, Gao L, Zhang W. Endoplasmic reticulum stress and autophagy participate in apoptosis induced by bortezomib in cervical cancer cells. *Biotechnol Lett.* 2016;38(2):357–65.
- Oh-Hashi K, Hasegawa T, Mizutani Y, Takahashi K, Hirata Y. Elucidation of brefeldin A-induced ER and Golgi stress responses in Neuro2a cells. *Mol Cell Biochem.* 2021;476(10):3869–77.
- Diaz-Corrales FJ, Miyazaki I, Asanuma M, Ruano D, Rios RM. Centrosomal aggregates and Golgi fragmentation disrupt vesicular trafficking of DAT. *Neurobiol Aging.* 2012;33(10):2462–77.
- Kishino A, Hayashi K, Maeda M, Jike T, Hidai C, Nomura Y, et al. Caspase-8 regulates endoplasmic reticulum stress-induced necroptosis independent of the apoptosis pathway in auditory cells. *Int J Mol Sci.* 2019;20(23):5896.
- Li J, Yakushi T, Parlati F, Mackinnon AL, Perez C, Ma Y, et al. Capzimin is a potent and specific inhibitor of proteasome isopeptidase Rpn11. *Nat Chem Biol.* 2017;13(5):486–93.
- Schimmer AD. Clisoquinol - a novel copper-dependent and independent proteasome inhibitor. *Curr Cancer Drug Targets.* 2011;11(3):325–31.
- Janen SB, Chaachouay H, Richter-Landsberg C. Autophagy is activated by proteasomal inhibition and involved in aggresome clearance in cultured astrocytes. *Glia.* 2010;58(14):1766–74.
- Kciuk M, Gielecinska A, Mujwar S, Kolat D, Kaluzinska-Kolat Z, Celik I, et al. Doxorubicin-an agent with multiple mechanisms of anticancer activity. *Cells.* 2023;12(4):659.
- Hao R, Nanduri P, Rao Y, Panichelli RS, Ito A, Yoshida M, et al. Proteasomes activate aggresome disassembly and clearance by producing unanchored ubiquitin chains. *Mol Cell.* 2013;51(6):819–28.
- Sha Z, Schnell HM, Ruoff K, Goldberg A. Rapid induction of p62 and GABARAP1 upon proteasome inhibition promotes survival before autophagy activation. *J Cell Biol.* 2018;217(5):1757–76.
- Fredrickson EK, Gardner RG. Selective destruction of abnormal proteins by ubiquitin-mediated protein quality control degradation. *Semin Cell Dev Biol.* 2012;23(5):530–7.
- Rosinol L, Oriol A, Rios R, Sureda A, Blanchard MJ, Hernandez MT, et al. Bortezomib, lenalidomide, and dexamethasone as induction therapy prior to autologous transplant in multiple myeloma. *Blood.* 2019;134(16):1337–45.
- Orlowski RZ, Nagler A, Sonneveld P, Blade J, Hajek R, Spencer A, et al. Randomized phase III study of pegylated liposomal doxorubicin plus bortezomib compared with bortezomib alone in relapsed or refractory multiple myeloma: combination therapy improves time to progression. *J Clin Oncol.* 2007;25(25):3892–901.

Publisher's Note

Springer Nature remains neutral with regard to jurisdictional claims in published maps and institutional affiliations.